V International Conference on Computational Methods for Coupled Problems in Science and Engineering
COUPLED PROBLEMS 2013
S. Idelsohn, M. Papadrakakis and B. Schrefler (Eds)

THE DRBEM SOLUTION OF THE GENERALIZED MAGNETO-THERMO-VISCOELASTIC PROBLEMS IN 3D ANISOTROPIC FUNCTIONALLY GRADED SOLIDS

MOHAMED ABDELSABOUR FAHMY*

* Faculty of Computers and Informatics
Suez Canal University
Old Campus, El-Sheikh Zayed, 41522 Ismailia, Egypt
e-mail: mafahmy2001@yahoo.com, http://mafahmy.webs.com/

Key words: Magneto-Thermo-Viscoelastic Problems, Green-Naghdi Theory, Functionally Graded Solids, Anisotropic, Dual Reciprocity Boundary Element Method.

Abstract. Our current problem is an important due to its many applications in modern aeronautics, astronautics, soil dynamics, geophysics, plasma physics, nuclear reactors and high-energy particle accelerators. It is hard to find the analytical solution of a problem in a general case, therefore, an important number of engineering and mathematical papers devoted to the numerical solution have studied the special cases of current general problem.
The basis of the boundary element method (BEM) is the transformation of the governing partial differential equations into a boundary integral equation. The presence of domain integrals in the BEM formulation implies domain discretization and this makes the BEM inefficient when compared with domain discretization techniques such as finite element method (FEM) or finite difference method (FDM). One of the most widely used techniques for converting the domain integral into a boundary one is the so-called dual reciprocity boundary element method (DRBEM), a numerical model based on the DRBEM taking into account the boundary and initial conditions is extended to solve the time-dependent generalized magneto-thermo-viscoelastic problems in anisotropic functionally graded solids. The unified formulation is tested through its application to the problem of a solid placed in a constant primary magnetic field. In the case of three-dimensional Cartesian coordinate system, a predictor-corrector implicit-implicit time integration algorithm was proposed and implemented for use with the DRBEM to obtain the temperature and displacement distributions with time in the context of the Green and Naghdi theory of type III. The results obtained are presented graphically in homogeneous and functionally graded materials.
The examples that appear in the literature using the Meshless Local Petrov-Galerkin (MLPG) method are special cases of our general problem. Also, there are alot of practical applications may be deduced as special cases from this general problem and may be implemented in commercial FEM software packages FlexPDE 6. In the considered special case, the results obtained with the DRBEM have been compared graphically with those obtained using the MLPG method and also the results obtained from the FlexPDE 6 are shown graphically in the same figures to confirm the validity of the proposed method. It can be seen from these figures that the DRBEM results are in excellent agreement with the results obtained by MLPG and FEM, thus confirming the accuracy of the DRBEM.

1 INTRODUCTION

Biot [1] introduced the theory of coupled thermoelasticity to overcome the first shortcoming in the theory of uncoupled thermoelasticity introduced by Duhamel [2] and Neuman [3] where it predicts two phenomena not compatible with physical observations. First, the equation of heat conduction of this theory does not contain any elastic terms. Second, the heat equation is of a parabolic type, predicting infinite speeds of propagation for heat waves. Later on, generalized theories of thermoelasticity were introduced in order to eliminate the shortcomings of the uncoupled thermoelasticity. Lord and Shulman (LS) [4] developed the theory of coupled thermoelasticity with one relaxation time by constructing a new law of heat conduction to replace the classical Fourier's law. This law contains the heat flux vector as well as its time derivative. It contains also new constant that acts as relaxation time. Since the heat equation of this theory is of the wave-type, it automatically ensures finite speeds of propagation for heat and elastic waves. Green and Lindsay (GL) [5] included a temperature rate among the constitutive variables to develop a temperature–rate-dependent thermoelasticity that does not violate the classical Fourier's law of heat conduction when the body under consideration has a center of symmetry; this theory also predicts a finite speed of heat propagation. This theory is known as the theory of thermoelasticity with two relaxation times. According to these theories, heat propagation should be viewed as a wave phenomenon rather than diffusion one. Relevant theoretical developments on the subject were made by Green and Naghdi (GN) [6, 7] they developed three models for generalized thermoelasticity of homogeneous isotropic materials which are labeled as model I, II and III. These theories of thermoelasticity LS, GL and GN theories are known as the generalized theories of thermoelasticity with finite thermal wave speed. In general, it is not easy to obtain analytical solutions of generalized magneto-thermo-visco-elastic problems in anisotropic functionally graded solids. Therefore, an important number of engineering and mathematical papers devoted to the numerical solution have studied the overall behavior of such materials [8-15].
The first step of the boundary element method (BEM) is the transformation of the physical problem at hand to an integral equation. Due to the pioneer work by Nardini and Brebbia [16], the boundary element method in conjunction with dual reciprocity method (DRM) and radial basis function (RBF), can now be used to obtain approximate solutions of general partial differential equation (PDE) systems. This strategy is often called as the dual reciprocity boundary element method (DRBEM). This method was initially developed in the context of two-dimensional (2D) elastodynamics and has been extended to deal with a variety of problems wherein the domain integral may account for linear-nonlinear static-dynamic effects. The DRBEM has been highly successful in a very wide range of engineering applications, including acoustics, aeroacoustics, aerodynamics, fluid dynamics, fracture analysis, geomechanics, elasticity and heat transfer. A more extensive historical review and applications of dual reciprocity boundary element method may be found in Refs. [17-20].

The main objective of this paper is to study the generalized magneto-thermo-viscoelastic problems in anisotropic solid of functionally graded material (FGM) in the context of the Green and Naghdi theory of type III. A predictor-corrector implicit-implicit time integration algorithm was developed and implemented for use with the dual reciprocity boundary element method (DRBEM) to obtain the solution for the temperature and displacement fields. The results obtained are presented graphically in homogeneous and functionally graded solids.

2 FORMULATION OF THE PROBLEM

Consider the coordinate system $Oxyz$ as shown in Fig. 1. We shall consider a functionally graded anisotropic solid placed in a primary magnetic field H_0 acting in the direction of the z-axis and occupies the region $R = \{(x, y, z): 0 < x < \underline{\gamma}, 0 < y < \underline{\beta}, 0 < z < \underline{\alpha}\}$ with graded material properties in the thickness direction (x-axis).

The governing equations of the generalized magneto-thermo-viscoelastic problems in the context of the Green and Naghdi theory of type III are given by [21]:

$$\sigma_{ab,b} + \tau_{ab,b} = \rho(x+1)^m \ddot{u}_a \tag{1}$$

$$\sigma_{ab} = \aleph(x+1)^m\left[C_{abfg}u_{f,g} - \beta_{ab}(T - T_0 + \tau_1\dot{T})\right], \aleph = \left(1 + \nu_0\frac{\partial}{\partial\tau}\right) \tag{2}$$

$$\tau_{ab} = \mu(x+1)^m\left(\tilde{h}_a H_b + \tilde{h}_b H_a - \delta_{ba}(\tilde{h}_f H_f)\right), \qquad \tilde{h}_a = \left(\nabla \times (\mathbf{u} \times \mathbf{H})\right)_a \tag{3}$$

$$k^*_{ab}T_{,ab} = -k_{ab}\dot{T}_{,ab} + \beta_{ab}T_0\ddot{u}_{a,b} + \rho c(x+1)^m\ddot{T}, \quad (k_{ab} = k_{ba}), (k_{12})^2 - k_{11}k_{22} < 0 \tag{4}$$

where σ_{ab} is the mechanical stress tensor, τ_{ab} is the Maxwell's electromagnetic stress tensor, u_k is the displacement, T is the temperature, $C_{abfg}\left(C_{abfg} = C_{fgab} = C_{bafg}\right)$ and $\beta_{ab}(\beta_{ab} = \beta_{ba})$ are respectively, the constant elastic moduli and stress-temperature coefficients of the anisotropic medium, $\aleph$ is the viscoelastic material constant, ν_0 is the viscoelastic relaxation time, μ is the magnetic permeability, $\tilde{h}$ is the perturbed magnetic field, k_{ab} are the thermal conductivity coefficients, ρ is the density, c is the specific heat capacity, τ is the time τ_1 is the mechanical relaxation time, m is a dimensionless constant and the traction vector can be written as

$$t_a = \sigma_{ab}n_b = \aleph(x+1)^m\left(C_{abfg}u_{f,g} - \beta_{ab}(T - T_0 + \tau_1\dot{T})\right)n_b \tag{5}$$

3 NUMERICAL IMPLEMENTATION

The field equations (1) and (4) can now be written in operator form as follows [22]:

$$L_{gb}u_f = f_{gb} \tag{6}$$

$$L_{ab}T = f_{ab} \tag{7}$$

in which

$$L_{gb} = D_{abf}\frac{\partial}{\partial x_b}, \qquad f_{gb} = \rho\ddot{u}_a - \left(D_aT + D_{af} + \Lambda D_{a1f}\right) \tag{8}$$

$$L_{ab} = k^*_{ab}\frac{\partial}{\partial x_a}\frac{\partial}{\partial x_b}, \qquad f_{ab} = -k_{ab}\dot{T}_{,ab} + \beta_{ab}T_0\ddot{u}_{a,b} + \rho c(x+1)^m\ddot{T} \tag{9}$$

where

$$D_{abf} = C_{abfg}\aleph\varepsilon, \varepsilon = \frac{\partial}{\partial x_g}, D_{af} = \mu H_0^2\left(\frac{\partial}{\partial x_a} + \delta_{a1}\Lambda\right)\frac{\partial}{\partial x_f}, \Lambda = \frac{m}{x+1},$$

$$D_a = -\beta_{ab}\left(\frac{\partial}{\partial x_b} + \delta_{b1}\Lambda + \tau_1\left(\frac{\partial}{\partial x_b} + \Lambda\right)\frac{\partial}{\partial\tau}\right)$$

Application of the weighted residual method (WRM) to Eq. (6), which, after integration by parts and use of the sifting property of the Dirac distribution, is written in the form of the following elastic integral representation formula

$$u_d(\xi) = \int_C (u_{da}^* t_a - t_{da}^* u_a + u_{da}^* \beta_{ab} T n_b)\, dC - \int_R f_{gb} u_{da}^* dR \tag{10}$$

By implementing the WRM and integration by parts using the sifting property, we obtain from (7) the thermal integral representation formula

$$T(\xi) = \int_C (q^* T - q T^*) dC - \int_R f_{ab} T^* dR \tag{11}$$

The thermoelastic representation formula (28) can be written in contracted notation as:

$$U_D(\xi) = \int_C \left(U_{DA}^* \mathrm{T}_A - \tilde{T}_{DA} U_A\right) dC - \int_R U_{DA}^* S_A dR \tag{12}$$

To transform the domain integral in (12) to the boundary, we approximate the source vector S_A in the domain by a series of given tensor functions f_{AN}^q and unknown coefficients α_N^q

$$S_A \approx \sum_{q=1}^{E} f_{AN}^q \alpha_N^q \tag{13}$$

Thus, the thermoelastic representation formula (12) can be written in the following form

$$U_D(\xi) = \int_C \left(U_{DA}^* T_A - \tilde{T}_{DA}^* U_A\right) d\mathrm{C} - \sum_{q=1}^{N} \int_R U_{DA}^* f_{AN}^q dR\, \alpha_N^q \tag{14}$$

The dual representation formulae of elastic and thermal fields can be combined as follows

$$U_{DN}^q(\xi) = \int_C \left(U_{DA}^* T_{AN}^q - T_{DA}^* U_{AN}^q\right) d\mathrm{C} - \int_R U_{DA}^* f_{AN}^q dR \tag{15}$$

With the substitution of (15) into (14), the dual reciprocity representation formula of coupled thermoelasticity can be expressed as follows

$$U_D(\xi) = \int_C \left(U_{DA}^* T_A - \check{T}_{DA}^* U_A\right) d\mathrm{C} + \sum_{q=1}^{N} \left(U_{DN}^q(\xi) + \int_C \left(T_{DA}^* U_{AN}^q - U_{DA}^* T_{AN}^q\right) dC \right) \alpha_N^q \tag{16}$$

According to the steps described in Fahmy [23], the dual reciprocity boundary integral equation (16) can be written in the following system of equations

$$\tilde{\zeta} \breve{u} - \eta \check{t} = \left(\zeta \breve{U} - \eta \breve{\wp}\right) \alpha \tag{17}$$

The generalized displacements U_F and velocities $\dot{U}_F$ are approximated by a series of tensor functions f_{FD}^q and unknown coefficients γ_D^q and $\tilde{\gamma}_D^q$ as follows [24]:

$$U_F \approx \sum_{q=1}^{N} f_{FD}^q(x)\gamma_D^q, \quad \dot{U}_F \approx \sum_{q=1}^{N} f_{FD}^q(x)\tilde{\gamma}_D^q \tag{18}$$

The same point collocation procedure described in Gaul, et al. [25] can be applied to (13) and (18). This leads to the following system of equations

$$\check{S} = J\alpha, \qquad U = J'\gamma, \qquad \dot{U} = J'\tilde{\gamma} \tag{19}$$

Now, the coefficients α can be expressed in terms of nodal values of the unknown displacements U, velocities $\check{\dot{U}}$ and accelerations $\check{\ddot{U}}$ as follows:

$$\alpha = J^{-1}\left(\left[\mathcal{B}^T J'^{-1} - \left(D_{af} + \Lambda D_{a1f}\right)\mho\right]U + \left[\left(k_{ab}\frac{\partial}{\partial x_a}\frac{\partial}{\partial x_b}\right)\delta_{AF}\right]\dot{U} + \left[\tilde{A} - c\rho(x+1)^m\delta_{AF}\right]\ddot{U}\right) \tag{20}$$

where $\mathcal{B}^T = \begin{cases} -D_a & A = 1,2,3; F = 4 \\ 0 & \text{otherwise} \end{cases}$, $\quad \tilde{A} = \begin{cases} \rho & A = 1,2,3;\ F = 1,2,3, \\ -T_0\beta_{fg}\varepsilon & A = 4;\ F = 4 \end{cases}$

$$\delta_{AF} = \begin{cases} -c\rho(x+1)^m & A = 4; F = 4 \\ 0 & \text{otherwise} \end{cases}$$

An implicit-implicit staggered algorithm was developed and implemented for use with the DRBEM for solving the governing equations which may now be written in a more convenient form after substitution of Eq. (20) into Eq. (17) as follows:

$$\overset{\frown}{M}\,\ddot{U} + \overset{\frown}{\Gamma}\,\dot{U} + \overset{\frown}{K}\,U = \overset{\frown}{\mathbb{Q}} \tag{21}$$

$$\overset{\frown}{\mathrm{X}}\,\ddot{T} + \overset{\frown}{\mathrm{A}}\,\dot{T} + \overset{\frown}{\mathrm{B}}\,T = \overset{\frown}{\mathbb{Z}}\,\ddot{U} \tag{22}$$

where $\overset{\frown}{M} = V\tilde{A}$, $\overset{\frown}{\Gamma} = V\left[\left(k_{ab}\frac{\partial}{\partial x_a}\frac{\partial}{\partial x_b}\right)\delta_{AF}\right]$, $\overset{\frown}{K} = \tilde{\zeta} + V\mathcal{B}^T J'^{-1} - \left(D_{af} + \Lambda D_{a1f}\right)\mho$, $\overset{\frown}{\mathbb{Q}} = \eta T$,

$\overset{\frown}{\mathrm{X}} = -\rho c(x+1)^m$, $\overset{\frown}{\mathrm{A}} = \left(k_{ab}\frac{\partial}{\partial x_a}\frac{\partial}{\partial x_b}\right)\delta_{AF}$, $\overset{\frown}{\mathrm{B}} = k_{ab}^*$, $\overset{\frown}{\mathbb{Z}} = T_0\beta_{ab}$, $V = \left(\eta\breve{\wp} - \zeta\breve{U}\right)J^{-1}$.

where $V, \overset{\frown}{M}, \overset{\frown}{\Gamma}$ and $\overset{\frown}{K}$ represent the volume, mass, damping and stiffness matrices, respectively, $\ddot{U}, \dot{U}, U, T$ and $\overset{\frown}{\mathbb{Q}}$ represent the acceleration, velocity, displacement, temperature and external force vectors, respectively, $\overset{\frown}{\mathrm{A}}$ and $\overset{\frown}{\mathrm{B}}$ are respectively the capacity and conductivity matrices, $\overset{\frown}{\mathrm{X}}$ is a vector of new material constants and $\overset{\frown}{\mathbb{Z}}$ is coupling matrix.
Hence the governing equations lead to the following coupled system of equations [26]:

$$\overset{\frown}{M}\,\ddot{U}_{n+1} + \overset{\frown}{\Gamma}\,\dot{U}_{n+1} + \overset{\frown}{K}\,U_{n+1} = \overset{\frown}{\mathbb{Q}}{}_{n+1}^{p} \tag{23}$$

$$\overset{\frown}{\mathrm{X}}\,\ddot{T}_{n+1} + \overset{\frown}{\mathrm{A}}\,\dot{T}_{n+1} + \overset{\frown}{\mathrm{B}}\,T_{n+1} = \overset{\frown}{\mathbb{Z}}\,\ddot{U}_{n+1} \tag{24}$$

where $\overset{\frown}{\mathbb{Q}}{}_{n+1}^{p} = \eta T_{n+1}^p$ and T_{n+1}^p is the predicted temperature. For further details, see the recent works of Fahmy [27-29].

Integrating Eq. (21) with the use of trapezoidal rule and Eq. (23), we have

$$\dot{U}_{n+1} = \dot{U}_n + \frac{\Delta\tau}{2}\left[\ddot{U}_n + \overset{\frown}{\widetilde{M}}^{-1}\left(\overset{\frown}{\widetilde{\mathbb{Q}}}{}^{p}_{n+1} - \overset{\frown}{\widetilde{\Gamma}}\,\dot{U}_{n+1} - \overset{\frown}{\widetilde{K}}\,U_{n+1}\right)\right] \tag{25}$$

$$U_{n+1} = U_n + \Delta\tau\dot{U}_n + \frac{\Delta\tau^2}{4}\left[\ddot{U}_n + \overset{\frown}{\widetilde{M}}^{-1}\left(\overset{\frown}{\widetilde{\mathbb{Q}}}{}^{p}_{n+1} - \overset{\frown}{\widetilde{\Gamma}}\,\dot{U}_{n+1} - \overset{\frown}{\widetilde{K}}\,U_{n+1}\right)\right] \tag{26}$$

From Eq. (25) we have

$$\dot{U}_{n+1} = \overline{\Upsilon}^{-1}\left[\dot{U}_n + \frac{\Delta\tau}{2}\left[\ddot{U}_n + \overset{\frown}{\widetilde{M}}^{-1}\left(\overset{\frown}{\widetilde{\mathbb{Q}}}{}^{p}_{n+1} - \overset{\frown}{\widetilde{K}}\,U_{n+1}\right)\right]\right] \tag{27}$$

where $\overline{\Upsilon} = \left(I + \frac{\Delta\tau}{2}\overset{\frown}{\widetilde{M}}^{-1}\overset{\frown}{\widetilde{\Gamma}}\right)$

Substituting from Eq. (27) into Eq. (26), we derive

$$U_{n+1} = U_n + \Delta\tau\dot{U}_n \tag{28}$$

$$+\frac{\Delta\tau^2}{4}\left[\ddot{U}_n + \overset{\frown}{\widetilde{M}}^{-1}\left(\overset{\frown}{\widetilde{\mathbb{Q}}}{}^{p}_{n+1} - \overset{\frown}{\widetilde{\Gamma}}\,\overline{\Upsilon}^{-1}\left[\dot{U}_n + \frac{\Delta\tau}{2}\left[\ddot{U}_n + \overset{\frown}{\widetilde{M}}^{-1}\left(\overset{\frown}{\widetilde{\mathbb{Q}}}{}^{p}_{n+1} - \overset{\frown}{\widetilde{K}}\,U_{n+1}\right)\right]\right] - \overset{\frown}{\widetilde{K}}\,U_{n+1}\right)\right]$$

Substituting $\dot{U}_{n+1}$ from Eq. (27) into Eq. (23) we obtain

$$\ddot{U}_{n+1} = \overset{\frown}{\widetilde{M}}^{-1}\left[\overset{\frown}{\widetilde{\mathbb{Q}}}{}^{p}_{n+1} - \overset{\frown}{\widetilde{\Gamma}}\left[\overline{\Upsilon}^{-1}\left[\dot{U}_n + \frac{\Delta\tau}{2}\left[\ddot{U}_n + \overset{\frown}{\widetilde{M}}^{-1}\left(\overset{\frown}{\widetilde{\mathbb{Q}}}{}^{p}_{n+1} - \overset{\frown}{\widetilde{K}}\,U_{n+1}\right)\right]\right]\right] - \overset{\frown}{\widetilde{K}}\,U_{n+1}\right] \tag{29}$$

Integrating the heat equation (22) using the trapezoidal rule, and Eq. (24) we get

$$\dot{T}_{n+1} = \dot{T}_n + \frac{\Delta\tau}{2}\left(\ddot{T}_{n+1} + \ddot{T}_n\right) = \dot{T}_n + \frac{\Delta\tau}{2}\left(\overset{\frown}{\widetilde{\mathrm{X}}}^{-1}\left[\overset{\frown}{\widetilde{\mathbb{Z}}}\,\ddot{U}_{n+1} - \overset{\frown}{\widetilde{\mathrm{A}}}\,\dot{T}_{n+1} - \overset{\frown}{\widetilde{\mathrm{B}}}\,T_{n+1}\right] + \ddot{T}_n\right) \tag{30}$$

$$T_{n+1} = T_n + \Delta\tau\dot{T}_n + \frac{\Delta\tau^2}{4}\left(\ddot{T}_n + \overset{\frown}{\widetilde{\mathrm{X}}}^{-1}\left[\overset{\frown}{\widetilde{\mathbb{Z}}}\,\ddot{U}_{n+1} - \overset{\frown}{\widetilde{\mathrm{A}}}\,\dot{T}_{n+1} - \overset{\frown}{\widetilde{\mathrm{B}}}\,T_{n+1}\right]\right) \tag{31}$$

From Eq. (30) we get

$$\dot{T}_{n+1} = \Upsilon^{-1}\left[\dot{T}_n + \frac{\Delta\tau}{2}\left(\overset{\frown}{\widetilde{\mathrm{X}}}^{-1}\left[\overset{\frown}{\widetilde{\mathbb{Z}}}\,\ddot{U}_{n+1} - \overset{\frown}{\widetilde{\mathrm{B}}}\,T_{n+1}\right] + \ddot{T}_n\right)\right] \tag{32}$$

where $\Upsilon = \left(I + \frac{1}{2}\overset{\frown}{\widetilde{\mathrm{A}}}\,\Delta\tau\,\overset{\frown}{\widetilde{\mathrm{X}}}^{-1}\right)$

Substituting from Eq. (32) into Eq. (31), we have

$$T_{n+1} = T_n + \Delta\tau\dot{T}_n + \tfrac{\Delta\tau^2}{4}\left(\ddot{T}_n + \overset{\frown}{\widetilde{\mathrm{X}}}^{-1}\left[\overset{\frown}{\widetilde{\mathbb{Z}}}\,\ddot{U}_{n+1}\right.\right. \tag{33}$$

$$\left.\left. -\overset{\frown}{\widetilde{\mathrm{A}}}\left(\Upsilon^{-1}\left[\dot{T}_n + \frac{\Delta\tau}{2}\left(\overset{\frown}{\widetilde{\mathrm{X}}}^{-1}\left[\overset{\frown}{\widetilde{\mathbb{Z}}}\,\ddot{U}_{n+1} - \overset{\frown}{\widetilde{\mathrm{B}}}\,T_{n+1}\right] + \ddot{T}_n\right)\right]\right) - \overset{\frown}{\widetilde{\mathrm{B}}}\,T_{n+1}\right]\right)$$

Substituting $\dot{T}_{n+1}$ from Eq. (32) into Eq. (24) we obtain

$$\ddot{T}_{n+1} = \widetilde{\mathrm{X}}^{-1}\left[\widetilde{\mathbb{Z}}\,\ddot{U}_{n+1} - \widetilde{\mathrm{A}}\left(\Upsilon^{-1}\left[\dot{T}_n + \frac{\Delta\tau}{2}\left(\widetilde{\mathrm{X}}^{-1}\left[\widetilde{\mathbb{Z}}\,\ddot{U}_{n+1} - \widetilde{\mathrm{B}}\,T_{n+1}\right] + \ddot{T}_n\right)\right]\right) - \widetilde{\mathrm{B}}\,T_{n+1}\right] \quad (34)$$

Now, a displacement predicted staggered algorithm for the solution of (28) and (33) is:
(1) Predict the displacement field: $U_{n+1}^{p} = U_n$.
(2) Substituting for $\dot{U}_{n+1}$ and $\ddot{U}_{n+1}$ from equations (25) and (23) respectively in Eq. (33) and solve the resulted equation for the temperature field.
(3) correct the displacement field using the computed temperature field for the Eq. (28).
(4) compute $\dot{U}_{n+1}$, $\ddot{U}_{n+1}$, $\dot{T}_{n+1}$ and $\ddot{T}_{n+1}$ from Eqs. (27), (29), (32) and (34) respectively.

4 NUMERICAL RESULTS AND DISCUSSION

For the purpose of numerical computations, the physical constants are as follows:
Elasticity tensor

$$C_{abfg} = \begin{bmatrix} 17.77 & 3.78 & 3.76 & 0.24 & -0.28 & 0.03 \\ 3.78 & 19.45 & 4.13 & 0 & 0 & 1.13 \\ 3.76 & 4.13 & 21.79 & 0 & 0 & 0.38 \\ 0 & 0 & 0 & 8.30 & 0.66 & 0 \\ 0 & 0 & 0 & 0.66 & 7.62 & 0 \\ 0.03 & 1.13 & 0.38 & 0 & 0 & 7.77 \end{bmatrix} \text{GPa}$$

Mechanical temperature coefficient and tensor of thermal conductivity are

$$\beta_{ab} = \begin{bmatrix} 0.001 & 0.02 & 0 \\ 0.02 & 0.006 & 0 \\ 0 & 0 & 0.05 \end{bmatrix} \cdot 10^6 \ \text{N/Km}^2, \qquad k_{ab} = \begin{bmatrix} 1 & 0.1 & 0.2 \\ 0.1 & 1.1 & 0.15 \\ 0.2 & 0.15 & 0.9 \end{bmatrix} \text{W/km}$$

Mass density $\rho = 2216\,\text{kg/m}^3$ and heat capacity $c = 0.1$ J/(kg K), $H_0 = 1000000$ Oersted, $\mu = 0.5$ Gauss/Oersted, $\aleph = 2$, $h = 2$, $\Delta\tau = 0.0001$.
The initial and boundary conditions considered in the calculations are:

$$\text{at } \tau = 0 \qquad \sigma_{ab} = \dot{\sigma}_{ab} = \tau_{ab} = \dot{\tau}_{ab} = 0,\ T = 0 \quad (35)$$

$$\text{at } x = 0 \qquad \frac{\partial u_1}{\partial x} = \frac{\partial u_2}{\partial x} = 0,\ \frac{\partial T}{\partial x} = 0, \qquad \text{at } x = \underline{\gamma} \qquad \frac{\partial u_1}{\partial x} = \frac{\partial u_2}{\partial x} = 0,\ \frac{\partial T}{\partial x} = 0 \quad (36)$$

$$\text{at } y = 0 \qquad \frac{\partial u_1}{\partial y} = \frac{\partial u_2}{\partial y} = 0,\ \frac{\partial T}{\partial y} = 0, \qquad \text{at } y = \underline{\beta} \qquad \frac{\partial u_1}{\partial y} = \frac{\partial u_2}{\partial y} = 0,\ \frac{\partial T}{\partial y} = 0 \quad (37)$$

$$\text{at } z = 0 \qquad \frac{\partial u_1}{\partial z} = \frac{\partial u_2}{\partial z} = 0,\ \frac{\partial T}{\partial z} = 0, \qquad \text{at } z = \underline{\alpha} \qquad \frac{\partial u_1}{\partial z} = \frac{\partial u_2}{\partial z} = 0,\ \frac{\partial T}{\partial z} = 0 \quad (38)$$

The results obtained are presented graphically in homogeneous solid (HS) and functionally graded solid (FGS), where we assumed that $m = 0.0$ in the HS case and $m = 0.5$ in the FGS case.
Figures 2 and 3 show the variation of the temperature T with time τ. We can conclude from these figures that the maximum temperature T occurs at $\tau = 3$ for FGS case. But it occurs at $\tau = 6$ for HS case.

Figures 4 and 5 illustrate the variation of the displacement u_1 with time τ. It can be seen that the maximum displacement u_1 occurs at $\tau = 3$ for the FGS case. But it occurs at $\tau = 6$ for the HS case.
Figures 6 and 7 show the variation of the displacement u_2 with time τ. It can be seen from the figures that the maximum displacement occurs in the FGS case. It can be noted from these figures that the displacement u_2 appears in an intense oscillation about a zero value, where the wave fronts collide with each other for the FGS case and may accumulate for the HS case.
Figures 8 and 9 illustrate the variation of the displacement $u_3$with time τ. It can be seen that the maximum displacement u_3 occurs at $\tau = 27.5$ for the HS case. But it occurs at $\tau = 18$ for the FGS case.
The present proposed method should be applicable to any three-dimensional generalized magneto-thermo-viscoelastic problem. The examples that appear in the literature using the Meshless Local Petrov-Galerkin (MLPG) method are special cases of our general problem. Also, there are alot of practical applications may be deduced as special cases from this general problem and may be implemented in commercial FEM software packages FlexPDE 6. In the considered special case of Hosseini et al. [30] who solved the special case from this study in the context of Green and Naghdi (GN) theory of type II, the results obtained with the DRBEM have been compared graphically, in figure 10, with those obtained using the MLPG method of Hosseini et al. [30] and also the results obtained from the FlexPDE 6 are shown graphically in the same figure to confirm the validity of the proposed method. It can be seen from this figure that the DRBEM results are in excellent agreement with the results obtained by MLPG and FEM, thus confirming the accuracy of the DRBEM.

5 CONCLUSION

In this paper, an algorithm to solve 3D generalized magneto-thermo-viscoelastic problems in anisotropic FGS was proposed and implemented for use with the DRBEM to obtain a solution for the displacement and temperature fields for both HS and FGS. Since there has been no previous solution is known for the current problem, the accuracy of the proposed algorithm was examined and confirmed by comparing the obtained results with those known previously from special cases of the present study. The DRBEM results are in excellent agreement with the special cases results obtained by MLPG method and FDM. So the proposed algorithm is very useful in solving 3D complex generalized magneto-thermo-viscoelastic problems.

REFERENCES

[1] Biot, M. Thermoelasticity and irreversible thermo-dynamics. J. Appl. Phys. (1956) 27:240-253.
[2] Duhamel, J. Some memoire sur les phenomenes thermo-mechanique. J. Ecole Polytech. (1837) 15:1-15.
[3] Neumann, F. Vorlesungen Uber die theorie der elasticitat, Meyer, Brestau, (1885).
[4] H.W. Lord, Y. Shulman, A generalized dynamical theory of thermoelasticity, J. Mech.

Phys. Solids (1967) 15:299-309.
[5] Green, A.E. Lindsay, K.A. Thermoelasticity, J. Elast. (1972) 2:1-7.
[6] Green, A.E. Naghdi, P.M. On undamped heat waves in an elastic solid. J. Therm. Stresses (1992) 15:253-264.
[7] Green, A.E. Naghdi, P.M. Thermoelasticity without energy dissipation, J. Elast. (1993) 31:189-208.
[8] Abd-Alla, A.M., El-Naggar, A.M. and Fahmy, M.A. Magneto-thermoelastic problem in non-homogeneous isotropic cylinder. Heat Mass Transfer (2003) 39:625-629.
[9] Abd-Alla, A.M., Fahmy, M.A. and El-Shahat, T.M. Magneto-thermo-elastic problem of a rotating non-homogeneous anisotropic solid cylinder. Arch. Appl. Mech. (2008) 78:135-148.
[10] Fahmy, M.A. Thermoelastic stresses in a rotating non-homogeneous anisotropic body. Numer. Heat Transfer, Part A (2008) 53:1001-1011.
[11] Fahmy, M.A. Influence of inhomogeneity and initial stress on the transient magneto-thermo-visco-elastic stress waves in an anisotropic solid. World J. Mech. (2011) 1:256-265.
[12] Fahmy, M.A. Numerical modeling of transient magneto-thermo-viscoelastic waves in a rotating nonhomogeneous anisotropic solid under initial stress. Int. J. Model. Simul. Sci. Comput. (2012) 3:125002.
[13] Fahmy, M.A. and El-Shahat, T.M. The effect of initial stress and inhomogeneity on the thermoelastic stresses in a rotating anisotropic solid. Arch. Appl. Mech. (2008) 78:431-442.
[14] El-Naggar, A.M., Abd-Alla, A.M., Fahmy, M.A. and Ahmed, S.M. Thermal stresses in a rotating non-homogeneous orthotropic hollow cylinder. Heat Mass Transfer (2002) 39:41-46.
[15] El-Naggar, A.M., Abd-Alla, A.M. and Fahmy, M.A. The propagation of thermal stresses in an infinite elastic slab. Appl. Math. Comput. (2004) 157:307-312.
[16] Nardini, D. and Brebbia, C.A. A new approach to free vibration analysis using boundary elements. in: Brebbia, C.A. (Eds.), Boundary elements in engineering, Springer, Berlin, (1982) 312-326.
[17] Brebbia, C.A., Telles, J.C.F. and Wrobel, L. Boundary element techniques in Engineering, Springer-Verlag, New York, (1984).
[18] Wrobel, L.C. and Brebbia, C.A. The dual reciprocity boundary element formulation for nonlinear diffusion problems. Comput. Methods Appl. Mech. Eng. (1987) 65:147-164.
[19] Fahmy, M.A. A time-stepping DRBEM for magneto-thermo-viscoelastic interactions in a rotating nonhomogeneous anisotropic solid. Int. J. Appl. Mech. (2011) 3:1-24.
[20] Fahmy, M.A. Transient magneto-thermoviscoelastic plane waves in a non-homogeneous anisotropic thick strip subjected to a moving heat source. Appl. Math. Modell. (2012) 36:4565-4578.
[21] Fahmy, M.A. Implicit-explicit time integration DRBEM for generalized magneto-thermoelasticity problems of rotating anisotropic viscoelastic functionally graded solids. Eng. Anal. Boundary Elem. (2013) 37:107-115.
[22] Fahmy, M.A. Transient magneto-thermo-elastic stresses in an anisotropic viscoelastic solid with and without moving heat source. Numer. Heat Transfer, Part A (2012) 61:547-564.

[23] Fahmy, M.A. A time-stepping DRBEM for the transient magneto-thermo-visco-elastic stresses in a rotating non-homogeneous anisotropic solid. Eng. Anal. Boundary Elem. (2012) 36:335-345.
[24] Partridge, P.W., Brebbia, C.A. and Wrobel, L.C. The dual reciprocity boundary element method. Computational Mechanics Publications, Boston, Southampton, (1992).
[25] Gaul, L., Kögl, M. and Wagner, M. Boundary element methods for engineers and scientists. Springer-Verlag, Berlin, (2003).
[26] Farhat, C., Park, K.C. and Dubois-Pelerin, Y. An unconditionally stable staggered algorithm for transient finite element analysis of coupled thermoelastic problems. Comput. Methods Appl. Mech. Eng. (1991) 85:349-365.
[27] Fahmy, M.A. The effect of rotation and inhomogeneity on the transient magneto-thermo-visco-elastic stresses in an anisotropic solid. ASME J. Appl. Mech. (2012) 79:051015.
[28] Fahmy, M.A. Generalized magneto-thermo-viscoelastic problems of rotating functionally graded anisotropic plates by the dual reciprocity boundary element method. J. Therm. Stresses (2013) 36:1-20.
[29] Fahmy, M.A. A three-dimensional generalized magneto-thermo-viscoelastic problem of a rotating functionally graded anisotropic solids with and without energy dissipation. Numer. Heat Transfer, Part A (2013) 63:713-733.
[30] Hosseini, S.M., Sladek, J. and Sladek, V. Meshless local Petrov-Galerkin method for coupled thermoelasticity analysis of a functionally graded thick hollow cylinder. Eng. Anal. Boundary Elem. (2011) 35:827-835.

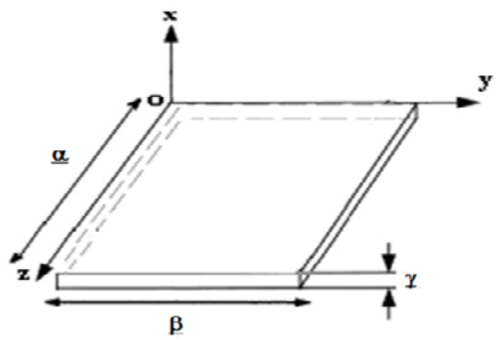

Fig. 1. The coordinate system of the solid.

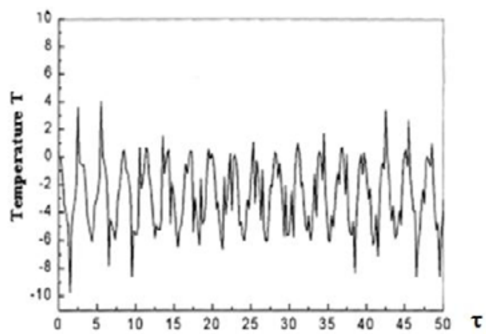

Fig. 2. Variation of the temperature T with time τ (HS).

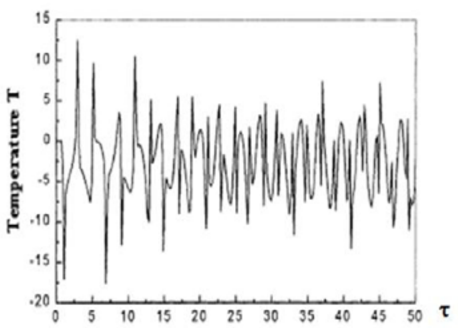

Fig. 3. Variation of the temperature T with time τ (FGS).

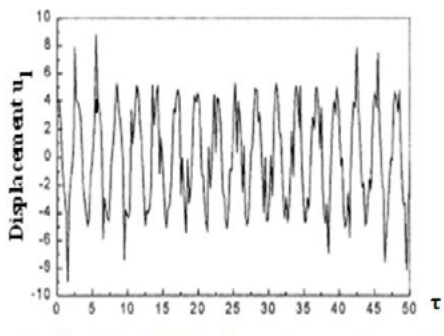

Fig. 4. Variation of the displacement u_1 with time τ (HS).

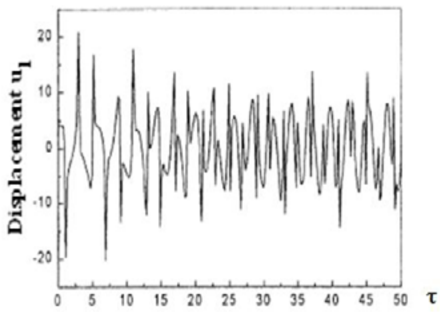

Fig. 5. Variation of the displacement u_1 with time τ (FGS).

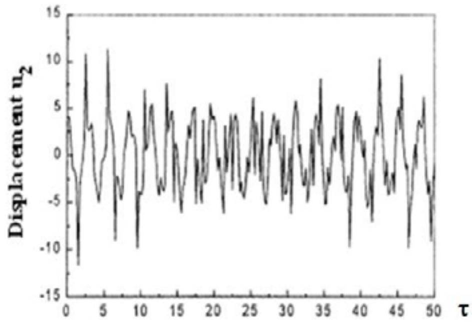

Fig. 6. Variation of the displacement u_2 with time τ (HS).

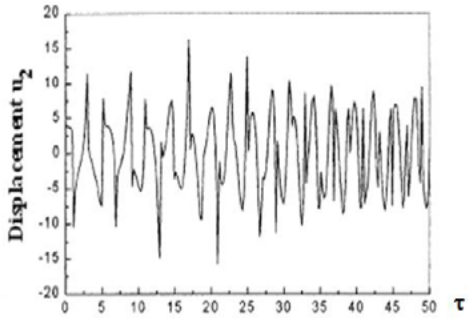

Fig. 7. Variation of the displacement u_2 with time τ (FGS).

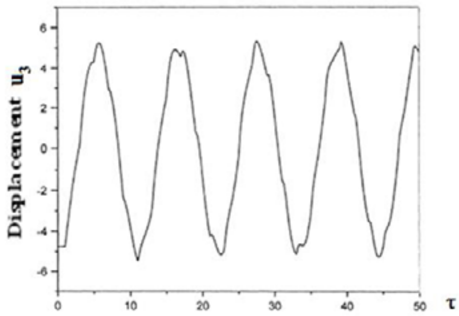

Fig. 8. Variation of the displacement u_3 with time τ (HS).

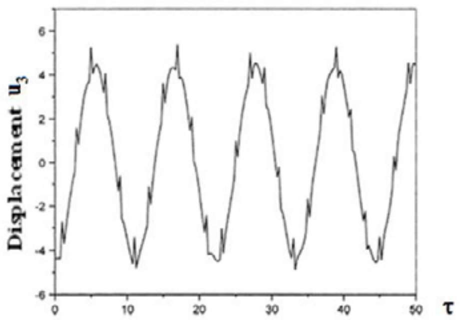

Fig. 9. Variation of the displacement u_3 with time τ (FGS).

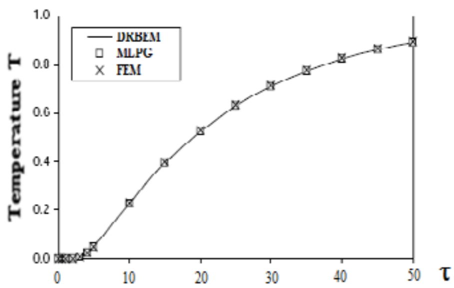

Fig. 10. Variation of the temperature T with time τ for three methods: DRBEM, MLPG, FEM.